Endocr (2009) 35:63–74
DOI 10.1007/s12020-008-9120-8

ORIGINAL PAPER

Ablation of NF-κB expression by small interference RNA prevents the dysfunction of human umbilical vein endothelial cells induced by high glucose

Gang Chen · Xiaoyan Shen · Jin Yao · Feng Chen · Xu Lin · Yufang Qiao · Tingting You · Fenghui Lin · Xiaowen Fang · Xin Zou · Lixiang Lin

Received: 28 July 2008 / Accepted: 10 October 2008 / Published online: 8 November 2008

Abstract Diabetes is a major independent risk factor for cardiovascular disease and stroke. High glucose (HG) reduces endothelial cell (EC) proliferation with a concomitant increase in apoptosis. HG also induces the translocation of nuclear factor (NF)-κB in human umbilical vein endothelial cells (HUVECs). However, data regarding the relationship between NF-κB signaling and HG-induced endothelial dysfunction are limited. In the present study, we constructed an NF-κB-targeting RNA interference (RNAi) adenovirus vector and cultured HUVECs in 5.5, 20.5, or 30.5 mM D-glucose or in daily alternating 5.5 or 30.5 mM D-glucose. We assessed the effects of the NF-κB pathway on proliferation under HG conditions by measuring bromodeoxyuridine incorporation and conducting methyl thiazolyltetrazolium assays. We also tested apoptosis by performing flow cytometry and terminal deoxynucleotidyl transferase nick-end labeling assay. The RNAi adenovirus effectively downregulated expression of the p65 protein in HUVECs for more than 6 days. Blockage of the NF-κB pathway with the RNAi adenovirus substantially protected HUVECs from decreased proliferation and reduced cellular apoptosis in HG conditions. These findings may explain how hyperglycemia promotes dysfunction of ECs and could elucidate a potential new target for therapeutic interventions.

This study had been approved by IRB of Fujian Provincial Hospital and all patients had signed the consent form.

G. Chen (✉) · X. Shen · J. Yao · F. Chen · Y. Qiao · T. You · F. Lin · X. Fang · X. Zou · L. Lin
Department of Endocrinology, Fujian Provincial Hospital, Fujian Medical University, 92 Huqian Road, Box 4-704, Fuzhou, Fujian, China
e-mail: chengang18@yahoo.com

X. Lin
Department of Molecular Medicine Research Center, Fujian Medical University, Fuzhou, China

Introduction

Diabetes mellitus is a major risk factor for cardiovascular complications and raises the risk of death threefold. Dysfunction of endothelial cells (ECs) is considered an early marker of such complications [1, 2]. Although diabetes and hyperglycemia induce multiple changes in metabolism and signaling, studies suggest that activation of the transcription factor nuclear factor (NF)-κB and chronic inflammation may be important features of secondary complications of diabetes [3]. NF-κB regulates apoptosis, proliferation, and inflammation in several cell types and is critical in the initiation and progression of the vascular complications of diabetes [4–6]. Moreover, the role of NF-κB signaling depends on the specific cell type and on the type of inducer [7]. Inhibition of proliferation and promotion of apoptosis are considered two major endothelial dysfunctions in high glucose (HG) conditions. We used a recombinant adenovirus expressing RNA interference (RNAi) specific to the gene for the p65 subunit of NF-κB to explore a possible role for the NF-κB pathway in regulating HG-induced proliferation and apoptosis of human umbilical vein endothelial cells (HUVECs).

Materials and methods

Materials

BLOCK-iT Adenoviral RNAi Expression System, Lipofectamine 2000, UltraPure agarose, a Western Brizee kit,

and a protein molecule ladder were obtained from Invitrogen Life Technologies (Carlsbad, CA). DMEM, medium 199, gelatin, Opti-MEM I reduced-serum medium, trypsin-EDTA (0.25%), nonessential amino acids, L-glutamine, and fetal bovine serum (FBS) were from Gibco-BRL. Hepes was purchased from Calbiochem. Rabbit anti-human factor VIII–related antigen polyclonal antibody was from Maixin Bioscience (Fuzhou, China). D-glucose, mouse anti-p65 antibody, and bromodeoxyuridine (BrdU) cell proliferation assay kits were acquired from Merck. High-Speed Plasmid Midi kits were obtained from Qiagen. Restriction enzyme PacI was from NEB. Penicillin, streptomycin, heparin, and endothelial-cell growth supplement were purchased from Sigma. Finally, 293A cells, TOP10 chemically competent *Escherichia coli*, and ccdB survival T1R chemically competent *E. coli* were from Invitrogen Life Technologies.

Construction of the NF-κB-targeting RNAi adenovirus vector

Cell culture

We cultured 293A cells in DMEM supplemented with 10% FBS, 0.1 mM nonessential amino acids, and 2 mM L-glutamine at 37°C in 5% CO_2 under 100% humidity. The cells were used to produce and amplify the adenovirus, as well as to titer adenoviral stocks.

Design and subcloning of short hairpin RNAs

Based on the p65 mRNA sequence from Genbank (NM 021975.2; GI:46430498), one RNAi starting point (1566) was selected to synthesize one pair of short hairpin RNA (shRNA) oligonucleotides. Two complementary oligonucleotides were designed on the basis of top strand 5′-CACCGGCTATAACTCGCCTAGTGACCGAAGTCACTAGGCGAGTTATAGCC-3′ and bottom strand 5′-AAAAGGCTATAACTCGCCTAGTGACTTCGGTCACTAGGCGAGTTATAGCC-3′.

Production and titering of adenovirus

Single-stranded oligonucleotides were annealed and ligated with linearized pENTR^{TM}/U6. The product was selected on agarose plates with kanamycin and characterized by PCR and sequencing to isolate correct clones. Isolated plasmid DNAs was named pEntry 1566. It was then recombined with an adenoviral backbone vector, and the recombinants were selected on agarose plates with ampicillin and then characterized by PCR. From clones double-selected on agarose plates with chloromycin and ampicillin, successfully recombined plasmid DNAs were isolated and named pAd 1566, while adenoviral backbone vector without recombination was named pAd-DEST.

The plasmids pAd1566 and pAd-DEST were digested by *Pac*I, purified, and transfected into HEK 293A cells using Lipofectamine 2000. Between 7 and 9 days after transfection, cytopathic effect (CPE) cells reached 80% of the total cells. Cells were then collected and freeze-thawed three times; the supernatant was the original virus solution. Viruses were amplified two times by infecting HEK 293A cells with the original virus solution. The supernatants of third generation viruses were collected and named Ad-DEST and Ad-1566, respectively. Virus titers were measured by plaque assay through infection of HEK 293A cells with the third generation viruses.

HUVEC isolation and culture conditions

HUVECs were isolated from umbilical cords resulting from normal pregnancies following the method of Jaffe et al. [8]. Cells were seeded on flasks coated with 0.1% gelatin in medium 199 supplemented with 20% FBS, penicillin 100 U/ml, 20 mmol/l Hepes, streptomycin 100 μg/ml, heparin 10 U/ml, and endothelial-cell growth supplement. Cells were grown at 37°C in a humidified 5% CO_2 incubator and subcultured at confluence by trypsinization with trypsin-EDTA. They were incubated with medium 199 supplemented with 10% FBS, penicillin 100 U/ml, streptomycin 100 μg/ml, and heparin 10 U/ml. ECs were identified by the presence of factor VIII-related antigen and a typical cobblestone appearance. ECs of the third to fifth passages in the actively growing condition were used for experiments. Medium was refreshed every 48 h, and 80% confluent cells were made quiescent in medium 199 supplemented with 1% FBS for 8 h before they were incubated under the various experimental conditions in the study, which are described next [3, 9].

Detection of p65 in HUVECs treated with the RNAi adenovirus

HUVECs were plated at a density of 2.0×10^6 cells/dish in 6-cm dishes (Corning). Levels of p65 protein were analyzed by means of Western blotting, as described previously [9]. In brief, cell lysates were prepared, electrotransferred, and immunoblotted with anti-p65 and anti-glyceraldehyde-3-phosphate dehydrogenase (GAPDH) polyclonal antibodies. Western blotting of GAPDH was performed to confirm that amounts of loaded proteins were equal. A range of multiplicities of infection (MOIs)—0, 5, 25, 50, 75, 100, and 150—was used to determine the optimal MOI for p65 knockdown at 60 h after infection. HUVECs were infected with adenovirus (Ad-DEST or Ad-1566) at MOI 50 and the cellular proteins were collected at 0, 24, 48, 72, 96, 120, and

144 h after infection. Western blots were conducted to monitor the p65 protein levels of HUVECs in response to adenoviral infection in terms of different viral MOI or time. Western blot signals were detected using a protein fluorescence detection kit (HyClone, Logan, UT) and X-ray film. Images were acquired by an image scanner (Amersham) and quantified by using its ImageQuant TLV2003 software.

Evaluation of the effects of the RNAi adenovirus on HG-induced translocation of NF-κB

Cells in the 6-cm dishes were made quiescent in medium 199 supplemented with 1% FBS for 8 h. They were then infected with Ad-1566/Ad-DEST for an additional 24 h before they were incubated with medium 199 plus 10% FBS and HG [normal glucose (NG) medium supplemented with glucose to a final concentration of 30.5 mM]. To clarify whether the Ad-1566/Ad-DEST influenced the effects of HG, we infected the cells with Ad-1566/Ad-DEST at MOI 50 for 24 h before exposing them to HG**.** Nuclear and cytoplasmic proteins were extracted using a kit (Beyotime Institute of Biotechnology, Jiangsu, China). In brief, after the cells were treated as indicated, cytosolic extracts were prepared by repeating cycles of freezing and thawing in 0.2 ml of cold buffer A. Nuclear protein was extracted by using ice-cold buffer C. Western immunoblotting was performed as described earlier. Values from three experiments for each treatment were used for statistical analysis.

Evaluation of the effects of HG conditions and the RNAi adenovirus on HUVECs under phase-contrast microscopy

We evaluated four groups: (i) continuous NG medium 5.5 mM + nontransduced HUVECs, (ii) continuous HG medium 30.5 mM + nontransduced HUVECs, (iii) continuous HG medium 30.5 mM + Ad-DEST groups HUVECs (negative shRNA control), and (iv) continuous HG medium 30.5 mM + Ad-1566 HUVECs. The cells were seeded on 6-well plates at 8.0×10^5 cells/cm^2. After subconfluence, the medium was changed to 800 μl medium 199 supplemented with 1% FBS with or without the adenovirus. Cells were incubated for 10 h, and then we added 1200 μl medium 199 supplemented with 16% FBS. On day 2, D-glucose was added to reach a final concentration of 30.5 mM in all groups except for the 5.5-mM group. Medium was changed every 48 h. Apoptotic cell death was monitored by means of morphologic analysis after 5 days (Fig. 2).

Methyl thiazolyltetrazolium assay

Cells were divided into NG and HG groups. HUVECs were plated at a density of 6000 cells/well on 96-well plates and incubated in medium 199 supplemented with 1% FBS for 8 h. After 24 h, we applied D-glucose 30.5 mM, and the cultures were incubated for 0, 1, 3, 5, 7, 9, or 10 days at 37°C. Thereafter, medium was changed every 48 h. Then, 100 μl of medium 199 was added to each well. We then added 10 μl of methyl thiazolyltetrazolium (MTT) to each well. After 4 h of incubation at 37°C, 100 μl of dimethyl sulfoxide was added to each well, and cells were incubated at 37°C overnight. Finally, optical densities were measured at 490 nm, and the growth inhibitory rate was calculated. Experiments were repeated three times.

BrdU cell-proliferation assay

The amount of BrdU incorporated into the cells was measured according to the manual for the kits. We seeded 150 μl of cells at a concentration of 10^5 cells/ml into a 96-well culture dish and then exposed them to the various experimental conditions for 5, 6, or 7 days. For the groups subjected to fluctuating conditions, glucose concentrations were changed every 24 h. We allowed the cells to incubate with BrdU for 12 h in the tissue-culture incubator. Then, this solution was removed, and 200 μl of the fixative/denaturing solution was added to each well. The cells were incubated for 30 min at room temperature. After thoroughly removing the solution, we added 100 μl of the anti-BrdU antibody (1:100) and incubated the cells for 1 h at room temperature. We washed the cells three times with 1× wash buffer. Peroxidase-labeled goat-anti-mouse IgG complex was added (1:1000; 100 μl/well) and incubated for 30 min at room temperature. Cells were then washed three times with wash buffer. Substrate was added (100 μl/well) and incubated in darkness for 15 min at room temperature. Afterward, termination buffer was added (100 μl/well) to terminate the reaction. Within 30 min, the absorptions at dual wavelengths 450–595 nm were measured.

Flow cytometry

Cells were trypsinized, counted, and seeded at 8.0×10^5 per well in 6-well plates until 80% confluence was achieved. Our five groups were (i) continuous NG medium 5.5 mM + nontransduced HUVECs, (ii) continuous HG medium 30.5 mM + nontransduced HUVECs, (iii) alternating HG and HG medium 30.5 mM + nontransduced HUVECs, (iv) continuous HG medium 30.5 mM + Ad-DEST HUVECs (negative shRNA control), and (v) continuous HG medium 30.5 mM + Ad-1566 HUVECs. After the groups were exposed to their respective conditions for 72 h, cells were harvested, pelleted, and washed with phosphate-buffered saline (PBS) and resuspended in PBS containing propidium iodide 20 mg/l and RNase A 1 mg/l. Fixed cells were examined for each experimental condition

with flow cytometry, and we determined the DNA divided by the total number of cells. The duration of exposure to HG was based on our previous observation and on the results of other studies [10]. All experiments were repeated three times.

Terminal deoxynucleotidyl transferase nick-end labeling assay

Four groups were assessed with terminal deoxynucleotidyl transferase nick-end labeling (TUNEL) assay: (i) continuous NG medium 5.5 mM + nontransduced HUVECs, (ii) continuous HG medium 30.5 mM + nontransduced HUVECs, (iii) continuous HG medium 30.5 mM + Ad-DEST HUVECs (negative shRNA control), and (iv) continuous HG medium 30.5 mM + Ad-1566 HUVECs. The cells were seeded on 6-well, gelatin-coated plates at 8.0×10^5 cells/cm^2. After preincubation with medium 199 supplemented with 1% FBS for 8 h, the Ad-DEST and Ad-1566 groups were infected with different RNAi adenovirus vectors at 50 MOIs. After 24 h, D-glucose was added to the medium for all groups except the 5.5-mM group. Medium was changed every 48 h. Then, the cells were exposed to the experimental conditions for 5 days. Finally, they were fixed in 0.14 M PBS (pH 7.4) containing 4% paraformaldehyde at 25°C for 60 min, washed in PBS three times for 5 min, and permeabilized in PBS containing 0.1% Triton X-100 and 0.1% sodium citrate at 4°C for 2 min.

The cells were washed and stained using the TUNEL reaction mixture (fluorescein-labeled deoxyuridine triphosphate and terminal deoxynucleotidyl transferase) at 37°C for 60 min in a humidified atmosphere in the dark. As a negative control, fixed and permeabilized cells were incubated with label solution instead of the TUNEL reaction mixture. In the positive control, cells were incubated with micrococcal nuclease before the labeling procedures. Samples were covered with parafilm or coverslips during incubation. The slides were rinsed three times with PBS. Samples were analyzed in a drop of PBS under a fluorescence microscope using an excitation wavelength in the range of 450 to 500 nm and detection in the range of 515 to 565 nm. The area around the sample was dried, and 50 µl of converter-AP was added to the sample and left at 37°C for 30 min. The slides were rinsed three times with PBS and incubated with substrate solution for 10 min at 15–25°C in the dark. They were again rinsed three times with PBS and analyzed under a light microscope.

Statistical analysis

Data are expressed as mean ± SD. Unpaired Student *t*-tests were used for comparisons between groups. For multiple comparisons, results were analyzed by means of analysis of variance followed by the least significance difference test. A *P*-value of <0.05 indicates a statistically significant difference.

Results

Construction and production of the RNAi adenovirus expression vector

PCR was used for identification of pEntry and pAd, pEntry was also sequenced. The result shows the size and open reading frame of pEntry1566 was correct. The correct recombination clones (pAd) were 600 bp. The sequence of the vector with the shRNA inserted was the same as designed by the software. Virus was titered by virus plaque assay. Results were 2.5×10^{10} pfu/ml for Ad-DEST and 3.0×10^9 pfu/ml for Ad-1566.

Verification of p65 gene silencing on Western blots

Results are shown in Fig. 1. Transduction with an empty vector (Ad-DEST) served as a control. Successful transduction was confirmed by immunoblotting with an anti-p65 antibody. Expression of p65 was significantly decreased in the Ad-1566 groups compared with the Ad-DEST groups ($P < 0.01$). In addition, we observed a dose-dependent reduction of p65 expression in the Ad-1566 groups ($P < 0.01$). Expression of p65 decreased in the MOI 5 group compared with the MOI 0 group, though the difference was not significant. Reductions in the expression of p65 were significant in cells infected with MOI 25 ($P < 0.05$), as well as for MOIs of 50, 75, 100, and 150 (all $P < 0.01$) compared with MOI 0. After MOI reached 75, there were no significant further reductions with increasing MOI. No significant differences were detected in the Ad-DEST groups at the different MOIs ($P > 0.05$). Therefore, we concluded that infection with Ad-1566 at MOI 25 began to lower expression of p65 and that it reached a peak at MOI 75. Because MOI 50 was sufficient to decrease expression of p65, further studies were done using that MOI.

We then looked for time-dependent reductions in p65 expression in the Ad-1566 groups at MOI 50. Transduction with an empty vector (Ad-DEST) served as a control. The results suggested marked time-dependent inhibition of p65 expression ($P < 0.01$). Expression was significantly decreased in the Ad-1566 groups compared with the Ad-DEST groups ($P < 0.01$). After 48 h, expression of p65 significantly decreased compared with nontransduction ($P < 0.01$). As observed in our previous research, the reduction did not significantly change after 96 h. No significant differences were detected in Ad-DEST groups at different times ($P > 0.05$). Therefore, we concluded that

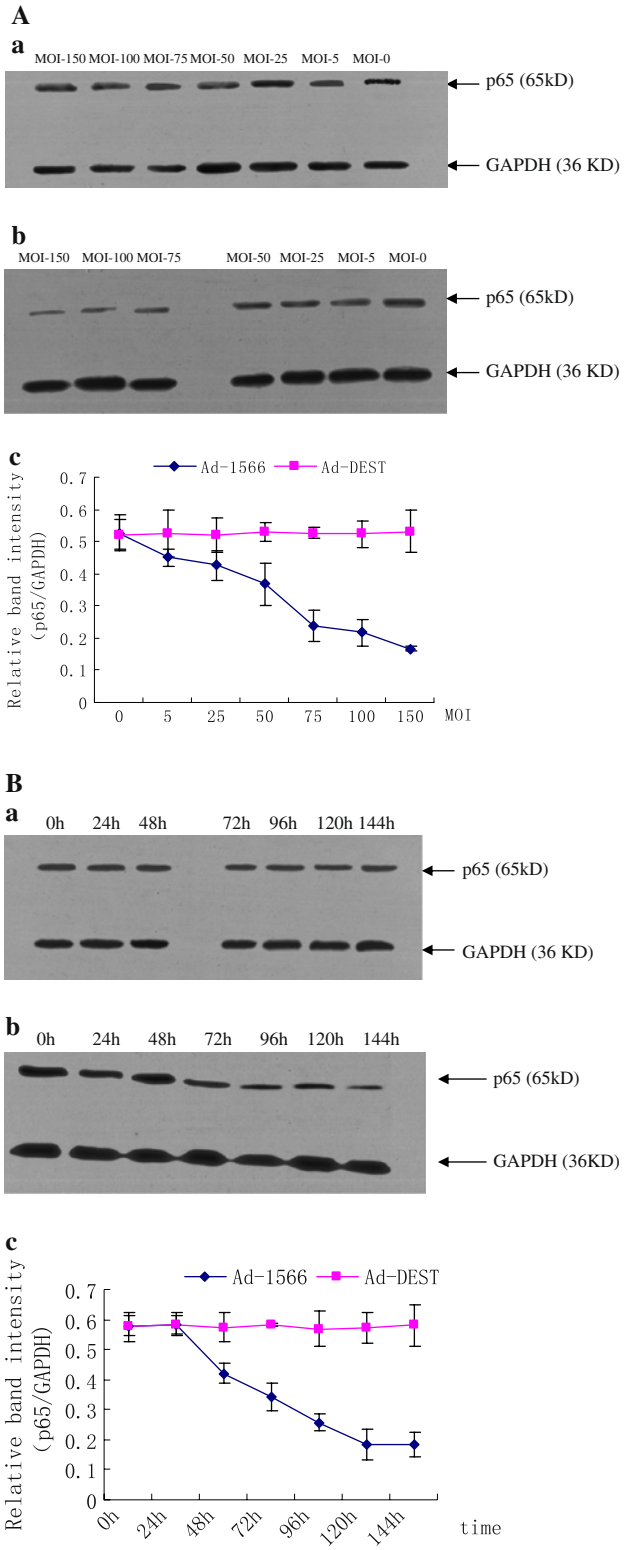

Fig. 1 Western blot analysis. Results represent three independent experiments. For different MOIs (**A**) and times (**B**), images show expression of total p65 protein in the Ad-DEST (**a**), Ad-1566 (**b**), and Ad-1566-Ad-DEST (**c**) groups

infection with Ad-1566 for 48 h decreased expression of p65. The Ad-1566 virus expressing an siRNA specific to p65 suppressed levels of p65 protein by 66.1–76.7% in HUVECs at day 6 after infection at MOI 50. In further research, we pretreated HUVECs with AD-1566 and Ad-DEST for 24 h before exposing them to glucose at MOI 50.

Effects of HG conditions and the RNAi adenovirus on HUVECs under phase-contrast microscopy

As previously described [10, 11], ECs exposed to HG show antiproliferative responses.

After 72 h of exposure to HG, the number of cells (85 ± 9.02) was significantly reduced to 65.37 ± 6.57% of NG group (130 ± 4.32) under microscope ($P < 0.01$). As Fig. 2 shows, some cells became round and eventually detached from the plate and floated in the medium, leaving many holes in the sheet of confluent cells after HG treatment. In addition, cells treated with HG exhibited characteristic features of cell shrinkage [12], membrane blebbing, and rounding, which were typical of apoptotic cell death. Preinfection with Ad-DEST did not alter the toxic effect of HG (the number of cells was 84 ± 9.09). However, apoptosis was significantly reduced after preinfection with Ad-1566 in the HG (the number of cells was 123 ± 9.71) compared with the HG group ($P < 0.01$).

Effects of RNAi adenovirus on HG-induced translocation of NF-κB

Signaling events that lead to NF-κB activation involve phosphorylation, ubiquitination, and proteolytic degradation of IκB-α from its inactive trimeric complex of IκB/p65/p50 in the cytosol. This is followed by translocation of the active dimmer (p65/p50) to the nucleus, where it binds to cognate DNA sequences to activate transcription [13].

Figure 3 shows the results of Western blotting of cytosolic and nuclear extracts to assess translocation of NF-κB to the nucleus to determine if ablation of NF-κB by siRNA affected signaling events. In the Ad-DEST study, incubation of HUVECs in HG 30.5 mM caused a time-dependent increase in nuclear protein ($P < 0.01$), which was maximal after 48 h and which remained at a similar level for at least up to 72 h (Fig. 3b). Similar results were obtained in a previous study [6], which suggested that the translocation of NF-κB p65 was independent of Ad-DEST. With Ad-1566, little translocation of NF-κB from the cytosol to the nucleus was observed (Fig. 3a, c). To further confirm the knockdown effect of Ad-1566 on the expression of p65 under HG conditions, we analyzed total cellular protein in the two groups. Total cellular protein consists of

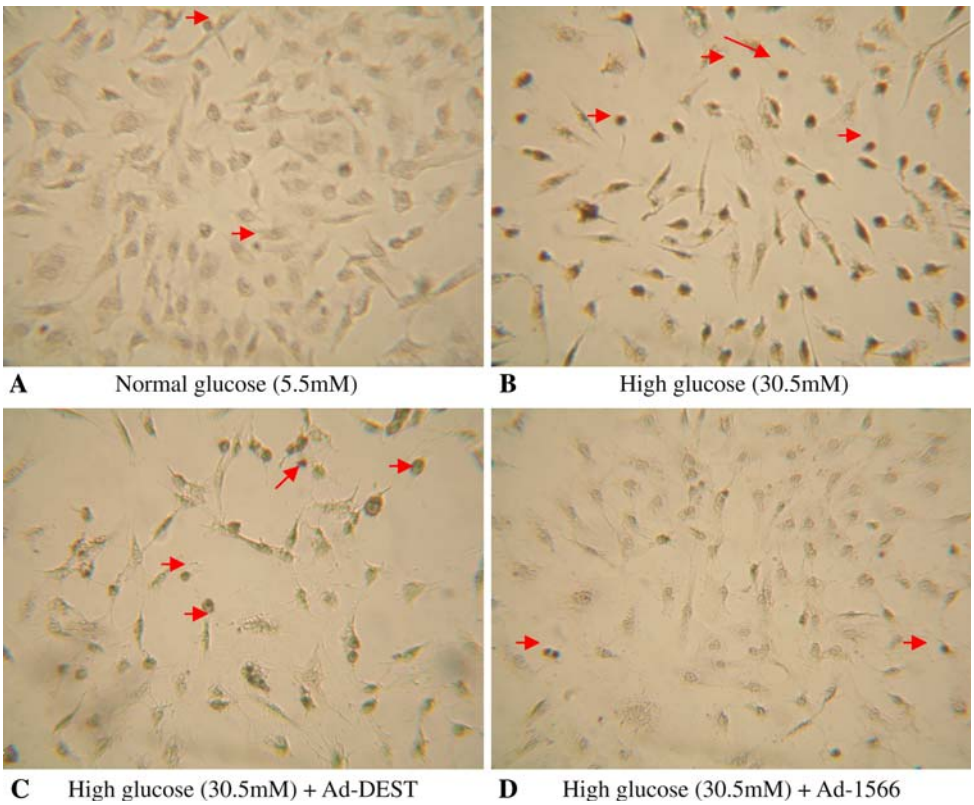

Fig. 2 Morphologic analysis of HUVECs cultured for 72 h with different concentrations of glucose and with or without the adenovirus expression vector. HUVECs were cultured in the presence of NG 5.5 mM (**a**), HG 30.5 mM (**b**), HG 30.5 mM + Ad-DEST (**c**), or HG 30.5 mM + Ad-1566 (**d**), as described in Materials and methods, then HUVECs were counted under microscope. Data are means ± SD of at least three independent experiments. *Arrows* indicate apoptotic features of nuclear pyknosis

cytoplasmic protein and protein in the nuclear extract. Treatment of HUVECs with Ad-1566 reduced total p65 protein by 74.51% after exposure to HG for 72 h (Fig. 3c).

Effects of HG conditions and/or p65 RNAi adenovirus on HUVEC proliferation

Baseline HUVEC proliferation in medium 199 containing 5.5 mM D-glucose followed standard growth kinetics with clearly defined lag (days 0–3), log (days 4–7), and plateau (day 8) phases (Fig. 4a). The number of proliferating HUVECs on days 5, 7, 9, and 10 was significantly lower when the cells were cultured in 30.5 vs. 5.5 mM D-glucose ($P < 0.05$ for day 5, for all others, $P < 0.01$, Fig. 4a). However, we found no difference in the rates of cell proliferation between the NG and HG groups within 3 days. To ascertain whether the decreased cell counts with 30.5 mM D-glucose were due to reduced proliferation or increased cell death, we performed flow cytometry with propidium iodide staining and a BrdU cell-proliferation assay.

As Fig. 4b shows, BrdU incorporation assays showed that DNA synthesis decreased in HUVECs exposed to HG 30.5 mM at all times, irrespective of the presence of stable or fluctuating glucose concentrations ($P < 0.01$). However, we observed no significant reduction in proliferation among HUVECs exposed to HG 20.5 mM on day 5 compared with NG group ($P > 0.05$). Intermittent HG produced effects worse than those of stable HG ($P < 0.05$) or NG ($P < 0.01$). In contrast, the concentration of glucose seemed less important than the presence of an alternating glucose level. Numbers of proliferating HUVECs on days 6 and 7 were similar when cells were cultured in 30.5 and 20.5 mM D-glucose ($P > 0.05$). On day 5, the increase in the concentration of glucose aggravated proliferative damage. Our results agree with previous findings that HG concentrations reduced proliferation in HUVECs [6]. Exposure to increasing concentrations of glucose diminished EC proliferation and lowered survival rates.

When grown in 30.5 mM D-glucose, the proliferation of HUVECs with Ad-1566 was significantly higher than that of HUVECs with Ad-DEST on days 5 and 6 ($P < 0.01$, Fig. 4c). On day 7, no increase was found in the knockdown groups ($P > 0.05$). Proliferation was significantly lower in HUVECs transduced with Ad-DEST than in nontransduced ECs at 30.5 mM D-glucose on days 5 and 6 ($P < 0.05$) but not day 7.

When we compared Ad-1566 ECs in 30.5 mM with nontransduced ECs in 30.5 or 5.5 mM D-glucose, protection was obvious. The Ad-1566 ECs proliferated more than nontransduced ECs in 30.5 mM D-glucose ($P < 0.01$, Fig. 4c) and as much as nontransduced ECs in 5.5 mM D-glucose ($P > 0.05$, Fig. 4c). NF-κB/p65-targeting RNAi adenovirus protected against proliferative impairment induced by 30.5 mM D-glucose and restored proliferation to control levels (5.5 mM D-glucose).

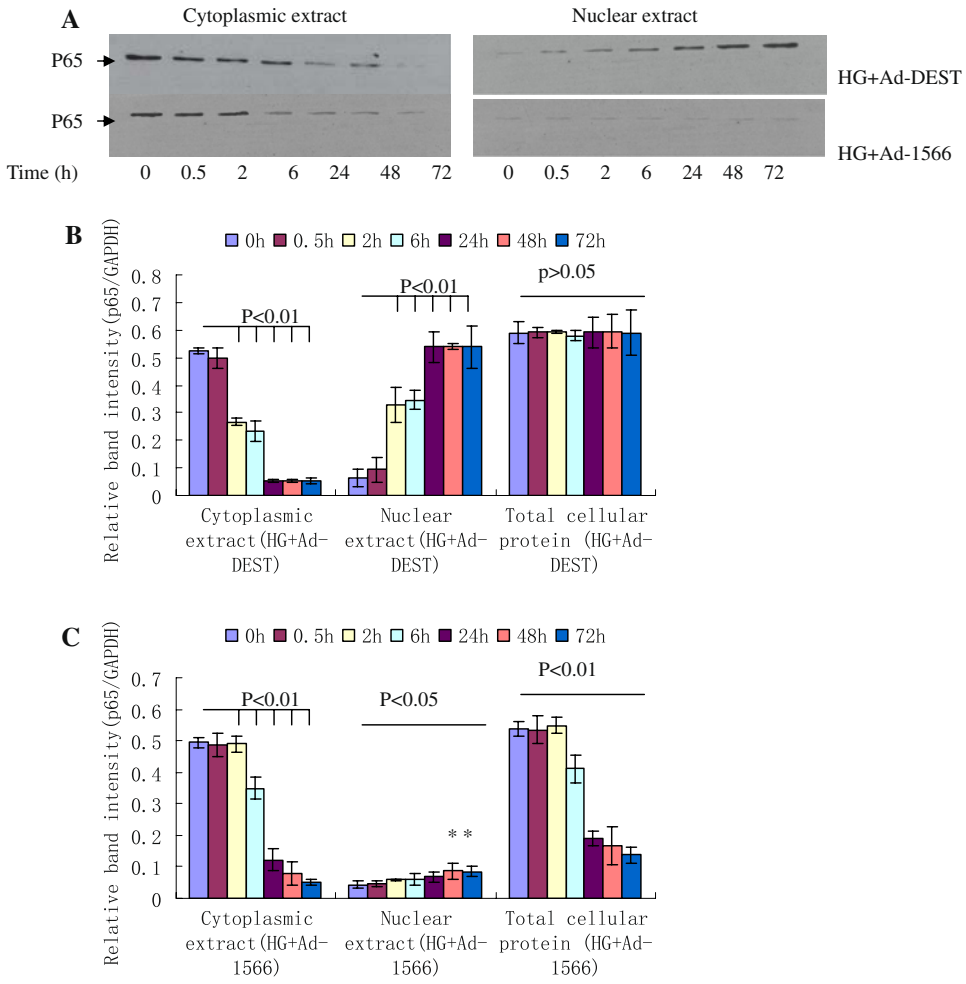

Fig. 3 Results of Western blotting. Representative blots show levels of cytoplasmic and nuclear p65 protein, with GAPDH (not shown), for adjusting differences in numbers of cells observed between treatments with HG 30.5 mM + Ad-DEST or Ad-1566 (**a**). Graphs summarize expression of cytoplasmic, nuclear, and total p65 protein in HG 30.5 mM + Ad-DEST (**b**) and HG 30.5 mM + Ad-1566 (**c**). *Asterisk* indicates the expression of nuclear p65 protein in HG 30.5 mM + Ad-1566 is significantly higher after 48 h

Results of flow cytometry

Because some have suggested that hyperglycemic spikes may play a substantial role in the pathogenesis of vascular diabetic complications [14], we explored the pro-apoptotic effort of fluctuating HG compared with stable HG., results were shown in Fig. 5.

Percentages of apoptotic cells significantly increased with fluctuating HG and stable HG compared with NG; respective values were, 35.6 ± 0.361, 25.57 ± 2.309, and 7.95 ± 2.286%.

In cells exposed to fluctuating concentrations of glucose, the percentage of apoptosis was as high as 35.2–35.9%. Intermittent HG enhanced apoptosis compared with stable HG ($P < 0.01$). Apoptosis was also evaluated for HUVECs in stable HG 30.5 mM pretreated with Ad-DEST or Ad-1566. Because empty vectors may exert a redundant effect on apoptosis, we performed the experiments with cells pretreated with Ad-DEST as a control. In the presence of Ad-DEST, the number of apoptotic cells did not change compared with incubation with HG alone ($P > 0.05$). However, the percentage of apoptotic cells decreased with Ad-1566 exposure ($P < 0.01$). Furthermore, the percentage did not significantly increase among cells treated with 30.5 mM glucose plus Ad-1566 *vs.* NG (11.10 ± 0.346 vs. 7.95 ± 2.286%, respectively, $P > 0.05$, Fig. 5c).

TUNEL staining

Compared with NG, HG significantly increased the number of TUNEL-positive cells (25.81 ± 1.773 vs. 8.20 ± 0.626%, $P < 0.05$, Fig. 6a, b). Incubation of HUVECs for 5 days in medium containing 30.5 mM of glucose plus the control vector vs. 30.5 mM of glucose showed no changes in TUNEL staining (26.10 ± 0.980 vs. 25.81 ± 1.773%, $P > 0.05$, Fig 6c, b). TUNEL staining decreased for ECs in 30.5 mM glucose plus Ad-1566 vs. ECs in 30.5 mM glucose plus Ad-DEST (11.49 ± 0.917 vs. 26.10 ± 0.980%, $P < 0.01$, Fig. 6d, c). HG stimulated apoptosis, and Ad-1566 protected HUVECs against apoptosis in vitro. However, the RNAi adenovirus specific for NF-kB p65 did not protect against apoptosis induced by 30.5 mM D-glucose to control levels (5.5 mM D-glucose) ($P < 0.01$). TUNEL staining significantly increased in ECs cultured in

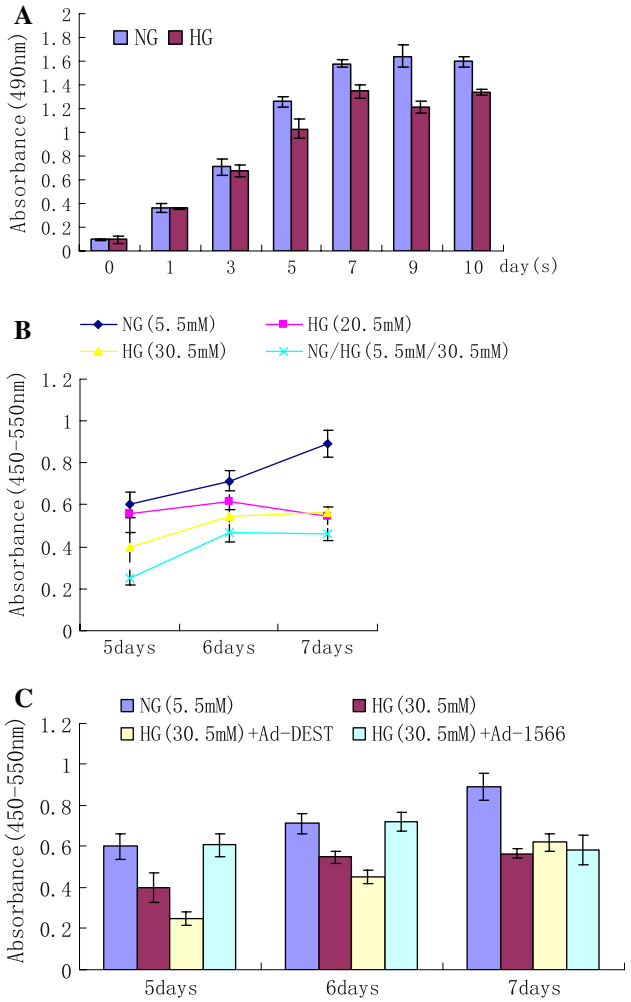

Fig. 4 Effects of HG and/or p65 RNAi adenovirus on HUVEC proliferation. (**a**) Absorbance after exposure to NG or HG medium on MTT assay (three experiments). The number of proliferating HUVEC on day 5, 7, 9, and 10 were significantly lower when cultured in 30.5 mM D-glucose than when cultured in 5.5 mM D-glucose. Analysis of stable or intermittent HG (**b**), as well as p65-targeting RNAi adenovirus Ad-1566 and the empty vector Ad-DEST (**c**) on proliferation on BrdU assay (at least three experiments). BrdU incorporation assays showed that DNA synthesis was decreased in HUVEC exposed to HG (30.5 mM) at any time point, irrespective of stable HG or fluctuating glucose ($P < 0.01$)

30.5 mM glucose plus Ad-1566 compared with ECs cultured in 5.5 mM glucose. Figure 6 shows representative images of TUNEL staining.

Discussion

Multicenter trials have demonstrated that intensive control of hyperglycemia can reduce the incidence or progression of microvascular complications of diabetes [15, 16]. In contrast, there is only limited data with respect to macrovascular complications such as ischemic heart disease, peripheral vascular disease, and thromboembolic stroke, which are major contributors to morbidity and mortality in diabetes. EC injury and proliferative dysfunction are considered the initial events in atherosclerosis, postangioplasty restenosis, plaque erosion, and thromboembolism [17], which contribute to macrovascular complications. Our results are consistent with these clinical observations. Most important of all,our data confirmed apoptosis and reduced proliferation in stable HG, furthermore showing that it was amplified in the fluctuating-glucose condition.

HG leads to reduced EC proliferation and concomitantly increased apoptosis [11, 14]. Risso et al. [14] reported that intermittent HG enhanced apoptosis in HUVECs, and Quagliaro et al. [18] further showed apoptosis of HUVECs exposed to intermittent HG may be related to a ROS overproduction, through PKC dependent activation of NAD(P)H oxidase, though how fluctuating HG affects proliferation of HUVECs has not been reported. The molecular mechanisms triggered by periodically changing glucose concentrations in cultured HUVECs are unknown. Metabolic variations induced by chronic exposure to HG might change or provide feed back to regulatory cellular controls, partially those counteracting the cytotoxic effects of glucose. Intermittent exposure to HG might reduce such an adaptation, causing pronounced toxicity. In addition, frequent fluctuations from high to low glucose levels jeopardize the antioxidant response of the cell and increase levels of oxidative stress markers, leading to higher cell damage than exposition to high constant glucose [19].

It is now recognized that glucose fluctuation per se is a strong predictor of cardiovascular disease [20]. Hyperglycemic spikes may play a notable role in the pathogenesis of vascular diabetic complications [21], and our data support the hypothesis that improved clinical outcomes may be related to efforts to decrease glucose fluctuations in patients with diabetes. In diabetic patients, the serum glucose concentration often changes markedly within a single day. By decreasing the duration and the degree of hyperglycemia, the aim of clinical diabetes care has been to slow the development of complications due to diabetes, and it has been shown that tightly controlling blood glucose levels by intensive treatment decreases the incidence of vascular complications in both types 1 and 2 diabetic patients [21].

To our surprise, when the concentration of glucose was higher than 20.5 mM, increasing it further did not alter proliferation. An increase from 20.5 to 30.5 mM did not further aggravate cellular dysfunction, at least in terms of the proliferative damage observed using the BrdU assay. Therefore, we speculate that too high a dose of glucose may not lead to progression of chronic vascular complications; rather, it may result in short-term complications, such as diabetic ketoacidosis, a hyperosmolar hyperglycemic state,

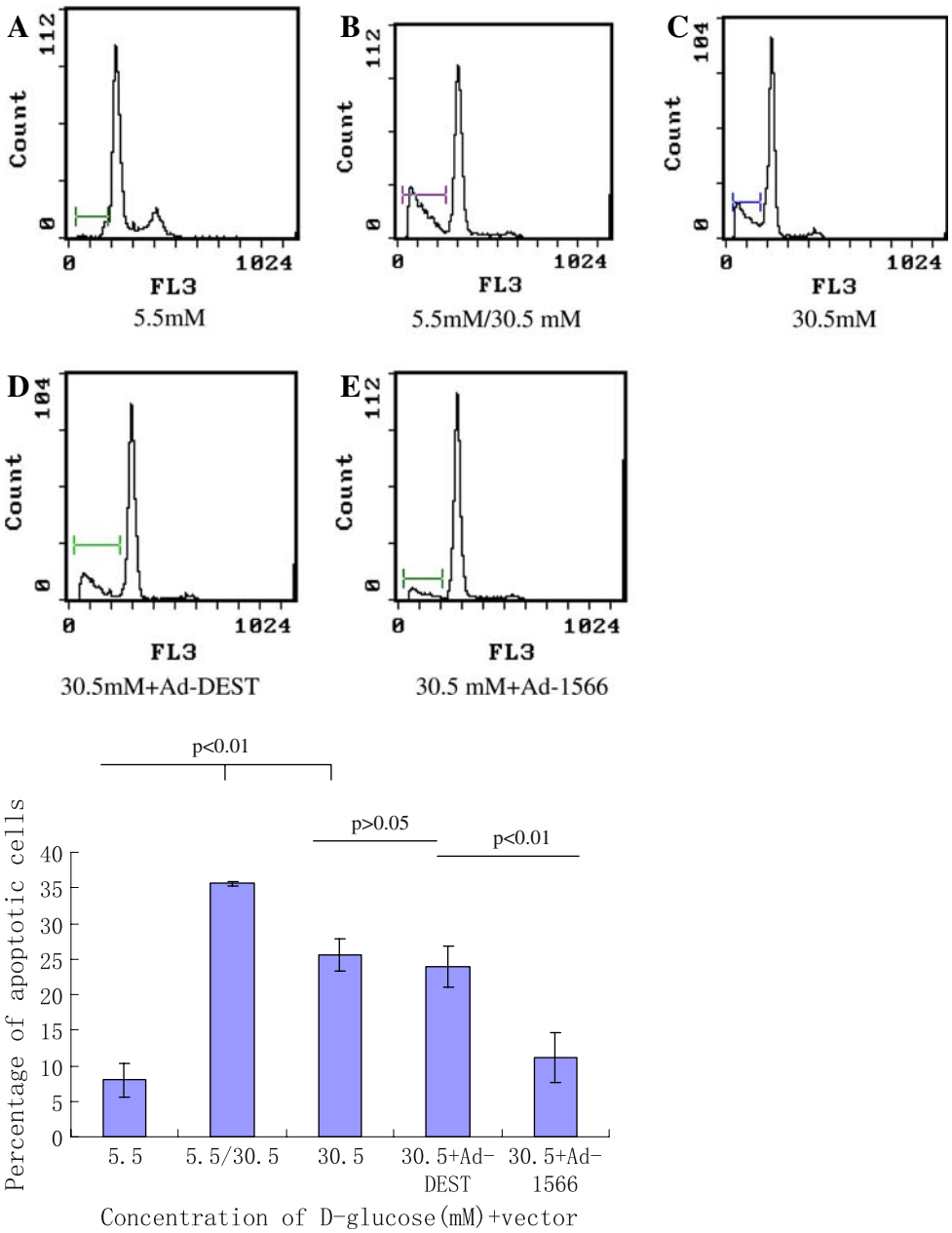

Fig. 5 Quantitative assessment of apoptosis in HUVECs by flow cytometry. HUVEC were divided into five groups: **a** Continous NG medium(5.5 mM) NG + untransduced HUVEC; **b** Continuous HG medium (30.5 mM) + untransduced HUVEC; **c** Alternating normal and HG medium (30.5 mM) + untransduced HUVEC; **d** Continuous HG medium (30.5 mM) + Ad-DEST groups (negative shRNA control) HUVEC, and (**e**) Continuous HG medium (30.5 mM) + Ad-1566 HUVEC. *Values* represent the average of three experiments. For 30.5 mM + Ad-1566 vs. 5.5 mM, $P > 0.05$

and lactic acidosis. To some extent, the concentration of glucose seemed less important than the presence of fluctuations in glucose. Further laboratory and clinical research must be carried out to confirm these findings.

Although the precise mechanisms underlying the aforementioned effects remain unclear, two lines of evidence suggest that NF-κB may mediate HG-induced dysfunction of ECs. First, NF-κB regulates expression of several genes important in the pathogenesis of diabetic complications [6, 22]. Second, NF-κB plays a critical role in regulating immune and inflammatory responses, cell growth, survival, and apoptosis [23–26]. Vascular tissues from patients with diabetes, as well as cultured cells exposed to HG, show increased binding of NF-κB to promoter regions of many inflammatory genes [27–31].

Some studies showed that NF-κB activation can prevent apoptosis in many cells types [32–35]. Investigators have reported that hyperglycemia enhances proliferation of HUVECs and that NF-κB activation may increase proliferation [36]. But in most studies, NF-κB activation produced, not prevented, apoptosis of ECs. However, to our knowledge, the role of NF-κB signaling in the context of hyperglycemia and EC proliferation has not been explored. In this study, we confirmed previous observations [5] and demonstrated, for the first time, that transduction with an NF-κB/p65-targeting RNAi adenovirus protected

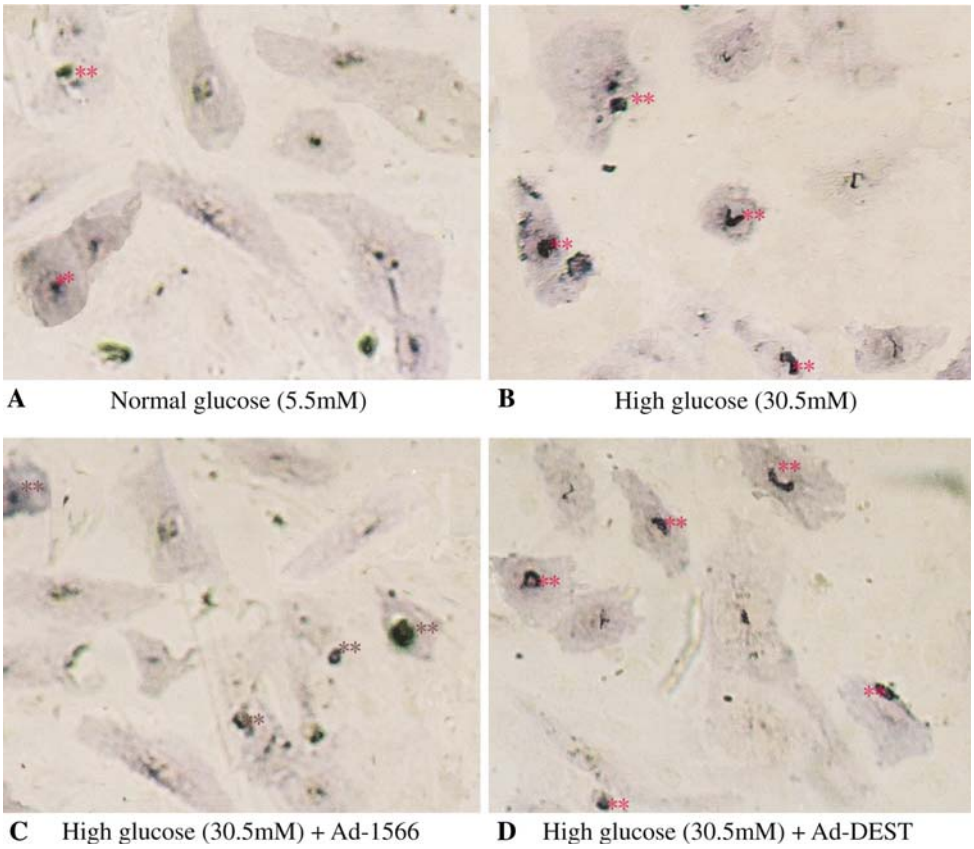

Fig. 6 Effect of the p65-targeting RNAi adenovirus Ad-1566 and the empty vector Ad-DEST on HG-induced EC apoptosis. Representative TUNEL stains of HUVECs cultured for 5 days with NG 5.5 mM (**a**), HG 30.5 mM (**b**), HG 30.5 mM + Ad-DEST (**c**), and HG 30.5 mM + Ad-1566 (**d**). *Asterisks* indicate nuclear pyknosis (TUNEL-positive cells). The results were quantified under phase-contrast microscopy

HUVECs from the apoptosis and inhibition of proliferation that is induced by HG.

Both in vivo and in vitro studies have demonstrated that HG activates NF-κB signaling by promoting translocation of nuclear p65, and that it may be a critical determinant of diabetic complications [37]. One study showed that inhibition of NF-κB can prevent the effects of HG on vascular smooth muscle cells in association with a decrease in the translocation of NF-κB from cytosol to nucleus [3]. Yozai et al. [38] reported that NF-κB activation of the renal cortex increased in diabetic rats compared with control rats and that methotrexate (MTX), an anti-inflammatory agent, could reverse the effect. In HUVECs, p65 protein in cytosolic extracts was significantly decreased in their HG cultures compared with NG, whereas p65 protein from nuclear extracts was significantly increased. MTX treatment of cells significantly inhibited the effect of HG on the translocation of NF-κB. However, researchers did not further investigate the relationship between NF-κB translocation and EC dysfunction. In our study, p65 protein from nuclear extracts significantly increased in control HG cultures but only slightly increased in the NF-κB-specific knockdown group, in which it was maintained at a low level.

HG initially increases the production of intracellular reactive oxygen species and activated NF-κB, and it mediates hyperglycemia-induced cellular damage in bovine ECs. Ho et al. [5, 39] tested the effects of pyrrolidine dithiocarbamate, an NF-κB inhibitor, and p65 NF-κB antisense oligonucleotide to clarify the role of NF-κB in HG-induced apoptosis in HUVECs. Pyrrolidine dithiocarbamate prevented apoptosis under HG conditions, and NF-κB antisense oligonucleotides suppressed HG-activated c-Jun N-terminal kinase (JNK) activity. In this way, some inhibitors can inactivate NF-κB and attenuate the development of atherosclerosis and its rapid progression. The significant inhibition of NF-κB translocation with MTX [38] is beneficial in treating diabetic nephropathy. However, degradation of IκB and adverse effects of MTX, including hepatotoxicity and nephrotoxicity, soon terminate its protective effects.

We report here that NF-κB mediates dysfunction of ECs due to HG. HG reduced EC proliferation, with a concomitant increase in apoptosis. Knockdown of NF-κB p65 reversed proliferative damage in HG 30.5 mM, even to the control level of 5.5 mM for at least 7 days after transduction. Meanwhile, it also reduced apoptosis of HUVECs under HG conditions. In conclusion, we demonstrated that the adverse effect of hyperglycemia on endothelial dysfunction is at least partly attributable to activation of NF-κB.

Shanmugam et al. [40, 41] and Figarola et al. [42] found that NF-κB regulates most genes induced by HG and that it

plays a central role in causing diabetic vascular and other complications. HG may mediate activation of NF-κB, which regulates expression of apoptosis- and proliferation-related genes in HUVECs.

Sequential activation of JNK mediates HG-induced apoptosis in HUVECs. In addition, NF-κB-specific antisense oligonucleotide suppresses HG-induced JNK activity [5, 39]. These results confirm that NF-κB-dependent activation of JNK is involved in HG-prompted HUVEC apoptosis. However, data on the relationship between NF-κB and HUVEC proliferation are limited. HG triggers reactive oxygen species-regulated NF-κB activation and proliferation in mesangial cells by means of a PI3k and Akt pathway [43]. Downregulation of phosphoinositide the 3-kinase/Akt pathway (PI3k and Akt) signaling pathways is responsible for proliferation inhibition under HG conditions [44]. HG results in sustained NF-κB activation with concomitant reduction of Akt survival signaling [5]. An emerging hypothesis is that protection from loss of proliferation involving Ad-1566 may be based on preventing reductions in PI3 K/Akt signaling. NF-κB may cross talk with JNK, as well as PI3 k and Akt signaling pathways in HG-induced EC dysfunction. In contrast, some have reported that activation of the PI3K/Akt signaling pathway is required for HG-induced activation of NF-κB mediated apoptosis in HUVECs [45]. The need for research, especially in vivo studies, into mechanisms dependent on NF-κB signaling must be emphasized.

Adenovirus is an important type of viral vector used in human gene therapy [46]. Adenoviral reagents that drive overexpression of selected genes have proven useful in both in vitro and in vivo metabolic research into diabetes and obesity [47]. Adenovirus is replication incompetent and does not stably integrate into cells. Hence, usage of adenoviruses may be a relatively safe approach to treat diseases. Nevertheless, they become diluted, and expression of p65 protein rebounds to normal levels when HUVECs divide. Our results indicated that NF-κB/p65-targeting RNAi adenovirus did not protect HUVECs from proliferation inhibition under HG conditions on day 8 after transduction. Our data also confirmed apoptosis and reduced proliferation in stable HG, furthermore showing that it was amplified in the fluctuating-glucose condition. The Ad-1566 protected HUVECs from dysfunction in the continuous HG. However, we failed to understand how the Ad-1566 prevented HUVECs from apoptosis and/or reduced proliferation in the intermittent HG. Further studies are needed to elucidate this point.

Acknowledgments This work was supported by Grant C071002 for natural science foundation from Fujian province of China and grant from the Ministry of Health of the People's Republic of China (WKJ 2005-2-021).

References

1. M.A. Gonzalez, A.P. Selwyn, Endothelial function, inflammation, and prognosis in cardiovascular disease. Am. J. Med. **115**(Suppl 8A), 99S–106S (2003)
2. B. Guerci, A. Kearney-Schwartz, P. Bohme, F. Zannad, P. Drouin, Endothelial dysfunction and type 2 diabetes. Part 1: physiology and methods for exploring the endothelial function. Diabetes Metab. **27**, 425–434 (2001)
3. K.V. Ramana, B. Friedrich, S. Srivastava, A. Bhatnagar, S.K. Srivastava, Activation of nuclear factor-κB by hyperglycemia in vascular smooth muscle cell is regulated by aldose reductase. Diabetes **53**, 2910–2920 (2004)
4. L. Li, T. Sawamura, G. Renier, Glucose enhances endothelial LOX-1 expression: role for LOX-1 in glucose-induced human monocyte adhesion to endothelium. Diabetes **52**, 1843–1850 (2003)
5. F.M. Ho, W.W. Lin, B.C. Chen, C.M. Chao, C.R. Yang, L.Y. Lin, C.C. Lai, S.H. Liu, C.S. Liau, High glucose-induced apoptosis in human vascular endothelial cells is mediated through NF-kappaB and c-Jun NH2-terminal kinase pathway and prevented by PI3K/Akt/eNOS pathway. Cell. Signal. **18**, 391–399 (2006)
6. S. Chen, S. Mukherjee, C. Chakraborty, S. Chakraborty, High glucose-induced, endothelin-dependent fibronectin synthesis is mediated via NF-κB and AP-1. Am. J. Physiol. Cell Physiol. **284**, C263–C272 (2003)
7. S. Ghosh, M.J. May, E.B. Koop et al., NF-κB and Rel protein: evolutionary conserved mediators of immune responses. Annu. Rev. Immunol. **16**, 225–260 (1998)
8. E.A. Jaffe, R.L. Nachman, C.G. Becker, C.R. Minick, Culture of human endothelial cells derived from umbilical veins. Identification by morphologic and immunologic criteria. J. Clin. Invest. **52**, 2745–2756 (1973)
9. H. Nakagami, R. Morishita, K. Yamamoto, S.I. Yoshimura, Y. Taniyama, M. Aoki, H. Matsubara, S. Kim, Y. Kaneda, T. Ogihara, Phosphorylation of p38 mitogen-activated protein kinase downstream of Bax-caspase-3 pathway leads to cell death induced by high D-glucose in human endothelial cells. Diabetes **50**, 1472–1481 (2001)
10. S. McGinn, P. Poronnik, E.D.M. Gallery, C.A. Pollock, High glucose and endothelial cell growth: novel effects independent of autocrine TGF-β1 and hyperosmolality. Am. J. Physiol. Cell Physiol. **284**, C1374–C1386 (2003)
11. S. McGinn, S. Saad, P. Poronnik, C.A. Pollock, High glucose-mediated effects on endothelial cell proliferation occur via p38 MAP kinase. Am. J. Physiol. Endocrinol. Metab. **285**, E708–E717 (2003)
12. F. Lang, M. Ritter, N. Gamper, S. Huber, S. Fillon, V. Tanneur, A. Lepple-Wienhues, I. Szabo, E. Gulbins, Cell volume in the regulation of cell proliferation and apoptotic cell death. Cell. Physiol. Biochem. **10**, 417–428 (2000)
13. D. Chandra, E.B. Jackson, K.V. Ramana, R. Kelley, S.K. Srivastava, A. Bhatnagar, Nitric oxide prevents aldose reductase activation and sorbitol accumulation during diabetes. Diabetes **51**, 3095–3101 (2002)
14. A. Risso, F. Mercuri, L. Quagliaro, G. Damante, A. Ceriello, Intermittent high glucose enhances apoptosis in human umbilical vein endothelial cells in culture. Am. J. Physiol. Endocrinol. Metab. **281**, E924–E930 (2001)
15. The Diabetes Control and Complications Trial Research Group, The effect of intensive treatment of diabetes on the development, and progression of long-term complications in insulin-dependent diabetes mellitus. N. Engl. J. Med. **329**, 977–986 (1993)
16. UK Prospective Diabetes Study Group, Intensive blood-glucose control with sulphonylureas or insulin compared with conventional

treatment, and risk of complications in patients with type 2 diabetes (U.KPDS 33). Lancet **352**, 837–853 (1998)
17. B.C. Berk, J.I. Abe, W. Min, J. Surapisitchat, C. Yan, Endothelial atheroprotective and anti-inflammatory mechanisms. Ann. N. Y. Acad. Sci. **947**, 93–109 (2001). discussion 109–111
18. L. Quagliaro, L. Piconi, R. Assaloni, L. Martinelli, E. Motz, A. Ceriello, Intermittent high glucose enhances apoptosis related to oxidative stress in human umbilical vein endothelial cells. The role of protein kinase C and NAD(P)H-oxidase activation. Diabetes **52**, 2796–2804 (2003)
19. L. Piconi, L. Quagliaro, R. Assaloni, R.D. Ros, A. Maier, G. Zuodar, A. Ceriello, Constant and intermittent high glucose enhances endothelial cell apoptosis through mitochondrial superoxide overproduction. Diabetes Metab. Res. Rev. **22**, 198–203 (2006)
20. M. Muggeo, G. Verlato, E. Bonora, G. Zoppini, M. Corbellini, R. de Marco, Long-term instability of fasting plasma glucose, a novel predictor of cardiovascular mortality in elderly patients with non-insulin-dependent diabetes mellitus. Circulation **96**, 1750–1754 (1997)
21. A. Ceriello, The emerging role of post-prandial hyperglycaemic spikes in the pathogenesis of diabetic complications. Diabet. Med. **15**, 188–193 (1998)
22. S. Majumdar, B.B. Aggarwal, Methotrexate suppresses NF kappaB activation through inhibition of IkappaB alpha phosphorylation and degradation. J. Immunol. **167**, 2911–2920 (2001)
23. C. Wadham, A. Parker, L. Wang, P. Xia, High glucose attenuates protein S-nitrosylation in endothelial cells: role of oxidative stress. Diabetes **56**(11), 2715–2721 (2007). Epub 2007 August
24. B.S. Zuckerbraun, C.A. McCloskey, R.S. Mahidhara, P.K. Kim, B.S. Taylor, E. Tzeng, Over expression of mutated IkappaBalpha inhibits vascular cap formation Smooth muscle cell proliferation and intimal hyperplasia formation. J. Vasc. Surg. **38**, 812–819 (2003)
25. J.M. Qin, X.M. Wan, J.Z. Zeng, M.C. Wu, Effect of Sirpalpha1 on the expression of nuclear factor-kappa B in hepatocellular carcinoma, Hepatobiliary Pancreat. Dis. Int. **6**, 276–283 (2007)
26. N. Nadiminty, J.Y. Chun, Y. Hu, S. Dutt, X. Lin, A.C. Gao, LIGHT, a member of the TNF superfamily, activates Stat3 mediated by NIK pathway. Biochem. Biophys. Res. Commun. **59**, 379–384 (2007)
27. L.J. Wang, X.P. Xing, A. Holmes, C. Wadham, J.R. Gamble, M.A. Vadas, P. Xia, Activation of the sphingosine kinase-signaling pathway by high glucose mediates the proinflammatory phenotype of endothelial cells. Circ. Res. **97**, 891–899 (2005)
28. M.J. Sheetz, G.L. King, Molecular understanding of hyperglycemia's adverse effects for diabetic complications. JAMA **288**, 2579–2588 (2002)
29. F. Chen, V. Castranova, X. Shi, New insights into the role of nuclear factor-kappaB in cell growth regulation. Am. J. Pathol. **159**, 387–397 (2001)
30. S. Chen, Z.A. Khan, M. Cukiernik, S. Chakrabarti, Differential activation of NF-κB and AP-1 in increased fibronectin synthesis in target organs of diabetic complications. Am. J. Physiol. **11**, 1089–1097 (2003)
31. P. Libby, Inflammation in atherosclerosis. Nature **420**, 868–874 (2002)
32. A.A. Beg, D. Baltimore, An essential role for NF-kappaB in preventing TNF-alpha-induced cell death. Science **274**, 782–784 (1996)
33. G. Tang, Y. Minemoto, B. Dibling, N.H. Purcell, Z. Li, M. Karin, A. Lin, Inhibition of JNK activation through NF-kappaB target genes. Nature **414**(6861), 265–266 (2001)
34. S. Wang, S. Kotamraju, E. Konorev, S. Kalivendi, J. Joseph, B. Kalyanaraman, Activation of nuclear factor-kappaB during doxorubicin-induced apoptosis in endothelial cells and myocytes is pro-apoptotic: the role of hydrogen peroxide. Biochem. J. **367**, 729–740 (2002)
35. R.E. Bellas, J.S. Lee, G.E. Sonenshein, Expression of a constitutive NF-kB-like activity is essential for proliferation of cultured bovine vascular smooth muscle cells. J. Clin. Invest. **96**, 2521–2527 (1995)
36. A. Sank, D. Wei, J. Reid, D. Ertl, M. Nimni, F. Weaver, A. Yellin, T.L. Tuan, Human endothelial cells are defective in diabetic vascular disease. J. Surg. Res. **57**, 647–653 (1994)
37. A. Bierhaus, S. Schiekofer, M. Schwaninger, M. Andrassy, P.M. Humpert, J. Chen, M. Hong, T. Luther, T. Henle, I. Kloting, M. Morcos, M. Hofmann, H. Tritschler, B. Weigle, M. Kasper, M. Smith, G. Perry, A.M. Schmidt, D.M. Stern, H.U. Haring, E. Schleicher, P.P. Nawroth, Diabetes-associated sustained activation of the transcription factor nuclear factor-κB. Diabetes **50**, 2792–2808 (2001)
38. K. Yozai, K. Shikata, M. Sasaki, A. Tone, S. Ohga, H. Usui, S. Okada, J. Wada, R. Nagase, D. Ogawa, Y. Shikata, M. Hirofumi, Methotrexate prevents renal injury in experimental diabetic rats via anti-inflammatory actions. J. Am. Soc. Nephrol. **16**, 3326–3338 (2005)
39. F.M. Ho, U.S.H. Li, C.S. Liau, P.J. Huang, S.Y. Lin-Shiau, High glucose-induced apoptosis in human endothelial cells is mediated by sequential activations of c-Jun NH2-terminal kinase and caspase-3. Circulation **101**, 2618–2624 (2000)
40. N. Shanmugam, Y.S. Kim, L. Lanting, R. Natarajan, Regulation of cyclooxygenase-2 expression in monocytes by ligation of the receptor for advanced glycation end products. J. Biol. Chem. **278**, 34834–34844 (2003)
41. N. Shanmugam, M.A. Reddy, M. Guha, R. Natarajan, High glucose-induced expression of proinflammatory cytokine and chemokine genes in monocytic cells. Diabetes **52**, 1256–1264 (2003)
42. J.L. Figarola, N. Shanmugam, R. Natarajan, S. Rahbar, Anti-inflammatory effects of the advanced glycation end product inhibitor LR-90 in human monocytes. Diabetes **56**, 647–655 (2007)
43. M.L. Sheu, F.M. Ho, K.F. Chao, M.L. Kuo, S.H. Liu, Activation of phosphoinositide 3-kinase in response to high glucose leads to regulation of reactive oxygen species-related nuclear factor-kappaB activation and cyclooxygenase-2 expression in mesangial cells. Mol. Pharmacol. **66**(1), 187–196 (2004)
44. S. Varma, B.K. Lal, R.F. Zheng, J.W. Breslin, S. Saito, P.J. Pappas, R.W. Hobson II, W.N. Dura′n, Hyperglycemia alters PI3 k and Akt signaling and leads to endothelial cell proliferative dysfunction. Am. J. Physiol. Heart Circ. Physiol. **289**, 1744–1751 (2005)
45. M.L. Sheu, F.M. Ho, R.S. Yang, K.F. Chao, W.W. Lin, S.Y.L. Shiau, S.H. Liu, High glucose induces human endothelial cell apoptosis through a phosphoinositide 3-kinase-regulated cyclooxygenase-2 pathway. Arterioscler. Thromb. Vasc. Biol. **25**(3), 539–545 (2005)
46. S. Arnhold, P. Heiduschka, H. Klein, Y. Absenger, S. Basnaoglu, F. Kreppel, S. Henke-Fahle, S. Kochanek, K.U. Bartz-Schmidt, K. Addicks, U. Schraermeyer, Adenovirally transduced bone marrow stromal cells differentiate into pigment epithelial cells and induce rescue effects in RCS rats. Invest. Ophthalmol. Vis. Sci. **47**(9), 4121–4129 (2005)
47. C.B. Newgard, While tinkering with the beta cell: metabolic regulatory mechanisms and new therapeutic strategies. Diabetes **51**, 3141–3150 (2002)